

Measurements of the triple-differential cross section for low-energy electron-impact ionization of argon

S. P. Hong and E. C. Beaty*

Joint Institute for Laboratory Astrophysics, University of Colorado and National Bureau of Standards, Boulder, Colorado 80309

(Received 1 December 1977)

The triple-differential cross section for electron-impact ionization of argon has been investigated for the primary electron energies near 100 eV and scattering angle 15° . The in-plane and out-of-plane measurements show that the forward lobe has a true minimum in the full three-dimensional sense when the ejected electron energy is 5 eV. However, such a minimum is not observed when the ejected electron energy is 20 eV. The cross section has much more structure than that of helium. No simple symmetry has been found common to all the cases for argon.

I. INTRODUCTION

In measurements of the triple-differential cross section all of the scattering parameters, except the spin, are experimentally determined. This provides the most detailed test of any theoretical approximation or model of electron-impact ionization. In recent years, much experimental work, especially for helium, has been reported.¹⁻¹⁹ For some measurements, the incident and two outgoing electrons are confined in one plane.¹⁻⁷ We will refer to these as in-plane measurements. For some other out-of-plane measurements, the two outgoing electrons are restricted to a symmetric configuration.⁸⁻¹³ In some cases, a full three-dimensional picture of the triple-differential cross section is essential to facilitate the test, and at present there are very few three-dimensional data available. Therefore it is the purpose of this work to report some measurements without the mechanical restrictions of most of the measurements reported previously. Since the accumulation of data for the triple-differential cross section is exceedingly slow and there are five independent variables involved, it is important to be very selective about data taking in this five-dimensional space. No theory so far is known to work well in the low-primary-energy range (from the threshold energy of the target gas to about 200 eV). More experimental data are apparently needed in order to refine the existing theories.²⁰⁻³³

Many theoretical calculations^{25,26,30-33} have been made to compare with the helium data. However, few calculations have been done for other target gases. One reason is the scarcity of experimental data for other gases in the low-incident electron-energy range. In this work, we choose to study the outer-shell ionization of argon for the primary electron energy near 100 eV and scattering angle 15° . The ground state of Ar^* is produced by removal of a $3p$ electron as contrasted with helium,

where a $1s$ electron is ejected. Hence argon is an interesting case to use to investigate the correlation between the triple-differential cross section and the state of the ejected electron.

II. EXPERIMENTAL APPARATUS

The details of the apparatus and the experimental procedures have already been discussed in our earlier papers.^{15,16} Therefore only a brief account will be given here. Figure 1 shows a conceptual diagram of the scattering quantities. The equipment essentially consists of four relatively independent systems which are directed at a small interaction region C . G , \vec{k}_0 , \vec{k}_a , and \vec{k}_b represent the gas beam and directions of incident and two outgoing-electron momenta, respectively.

The gas beam is formed by a multichannel array. The size of the gas beam is about 3.5 mm full width at half maximum (FWHM). The gas pressure in the scattering center is an order of magnitude higher than the background pressure which is about 2×10^{-5} Torr.

The electron gun with a tungsten wire filament and cylindrical lenses of molybdenum can be rotated horizontally about a vertical axis through the center of the gas beam. The electron beam is

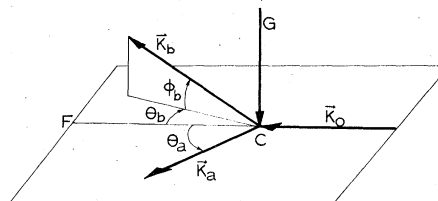


FIG. 1. Conceptual diagram of the scattering quantities. G is the direction of gas beam. \vec{k}_0 , \vec{k}_a , and \vec{k}_b show the directions of the incident and two outgoing electrons. F shows the location of the Faraday cup and C indicates the scattering center.

about 2 mm in diameter with an energy spread of about 0.3 eV. The beam is directed into a deep Faraday cup and the current is about 40 nA.

Of the two outgoing electrons, we refer to the one with higher energy (\vec{k}_a) as the scattered electron, and the one with lower energy (\vec{k}_b) as the ejected electron. The plane containing the incident and scattered electrons is called scattering plane. An electron analyzer collects the scattered electrons from the interaction region and counts those which meet appropriate specifications on direction and energy. Energy selection is made with a hemispherical deflector with an energy resolution about 0.6 eV FWHM and an angular resolution of 1° . Individual electrons are counted by a channel electron multiplier. The scattered-electron analyzer is fixed with respect to the vacuum system. The axis of this analyzer is horizontal and provides a convenient reference for measuring the angular position of the gun. We call the angle between the axis of the gun and that of the scattered-electron analyzer θ_a , or the scattering angle (see Fig. 1).

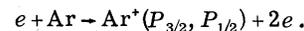
A time-of-flight analyzer detects ejected electrons from the interaction region which meet selected specifications on angle. It accepts a broad band of energies, with very-low-energy electrons rejected by a retarding lens. The electron multiplier used is capable of a high count rate. This detector can be moved about two orthogonal axes. Position is indicated by two angles θ_b and ϕ_b (see Fig. 1). The angular resolution of the time-of-flight analyzer is 2.5° . Both of the electron analyzers are designed to have a field of view big

enough to encompass the entire interaction region.

True coincidence events can be distinguished by the fact that the electrons from the same ionization event will have a definite amount of time delay between their arrivals, while the electrons from different ionization events have a uniform delay spectrum. Typically 1–100 true coincidence counts per minute are collected. The multichannel analysis is done by a small computer which, also under program control, sets the angles θ_a , θ_b , and ϕ_b . A table of angles is scanned several times to permit a reproducibility check and to minimize the effects of instrumental drift. The total counting time for a fixed set of angle variables is about 1–3 h.

III. RESULTS

The electron-impact ionization of argon presently under study can be represented by



The spin-orbit interaction in the ground state of Ar^* causes a doublet separated by about 177 meV. At present, these two states are not resolved. Hence our measured triple-differential cross section contains the contributions from the transitions to both of these two states.

The experimental data presented here are for two sets of energy variables. The primary electron energy E_0 is 100 eV and the ejected electron energy E_b is 5 eV for the first set. E_0 and E_b are 115 and 20 eV, respectively, for the second set. For both sets of data the scattering angle θ_a is

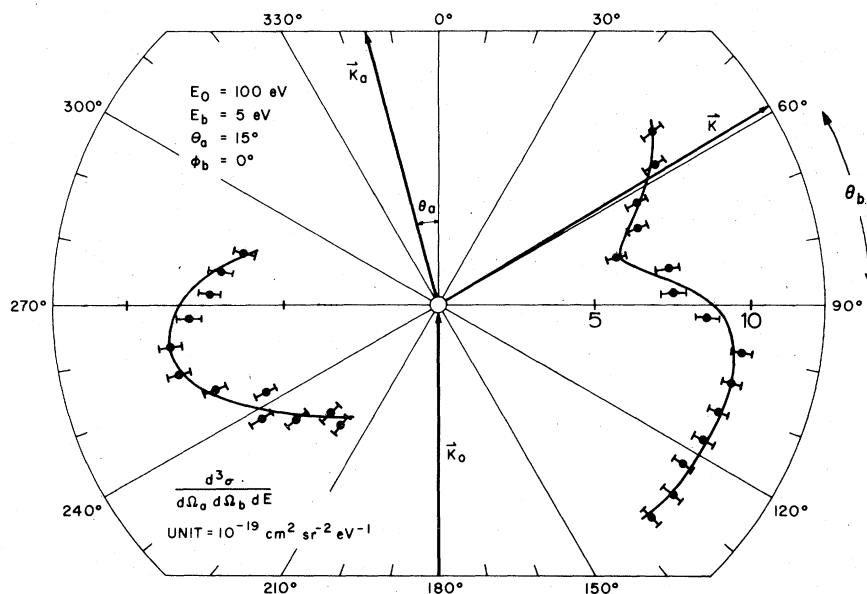


FIG. 2. In-plane triple differential cross section ($\phi_b = 0$) of argon as a function of detection angle θ_b of the ejected electrons are presented in polar coordinate. This is the result for the case where $E_0 = 100$ eV, $E_b = 5$ eV, and $\theta_a = 15^\circ$. \vec{k}_0 , \vec{k}_a , and \vec{k}_b indicate the directions of incident scattered electrons and momentum transfer, respectively. Dots are the experimental data points. The error bars stand for one standard deviation. The curves are the lines fitting those data points to outline the shape of the triple-differential cross section.

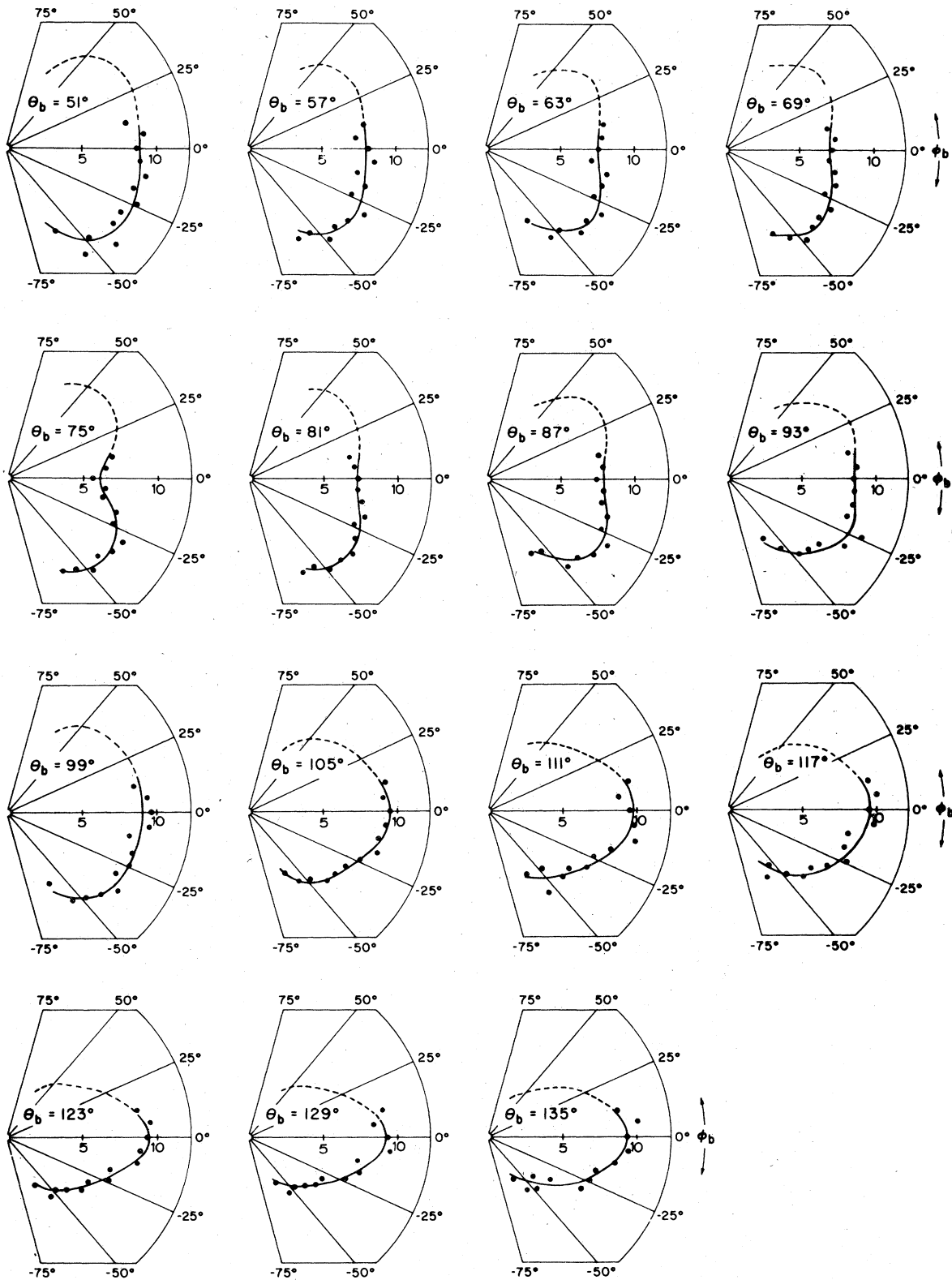


FIG. 3. Vertical scans of the forward lobe with θ_b from 51° to 135° in every 6° interval, for the case where $E_0 = 100$ eV, $E_b = 5$ eV, and $\theta_a = 15^\circ$. Units are the same as in Fig. 2.

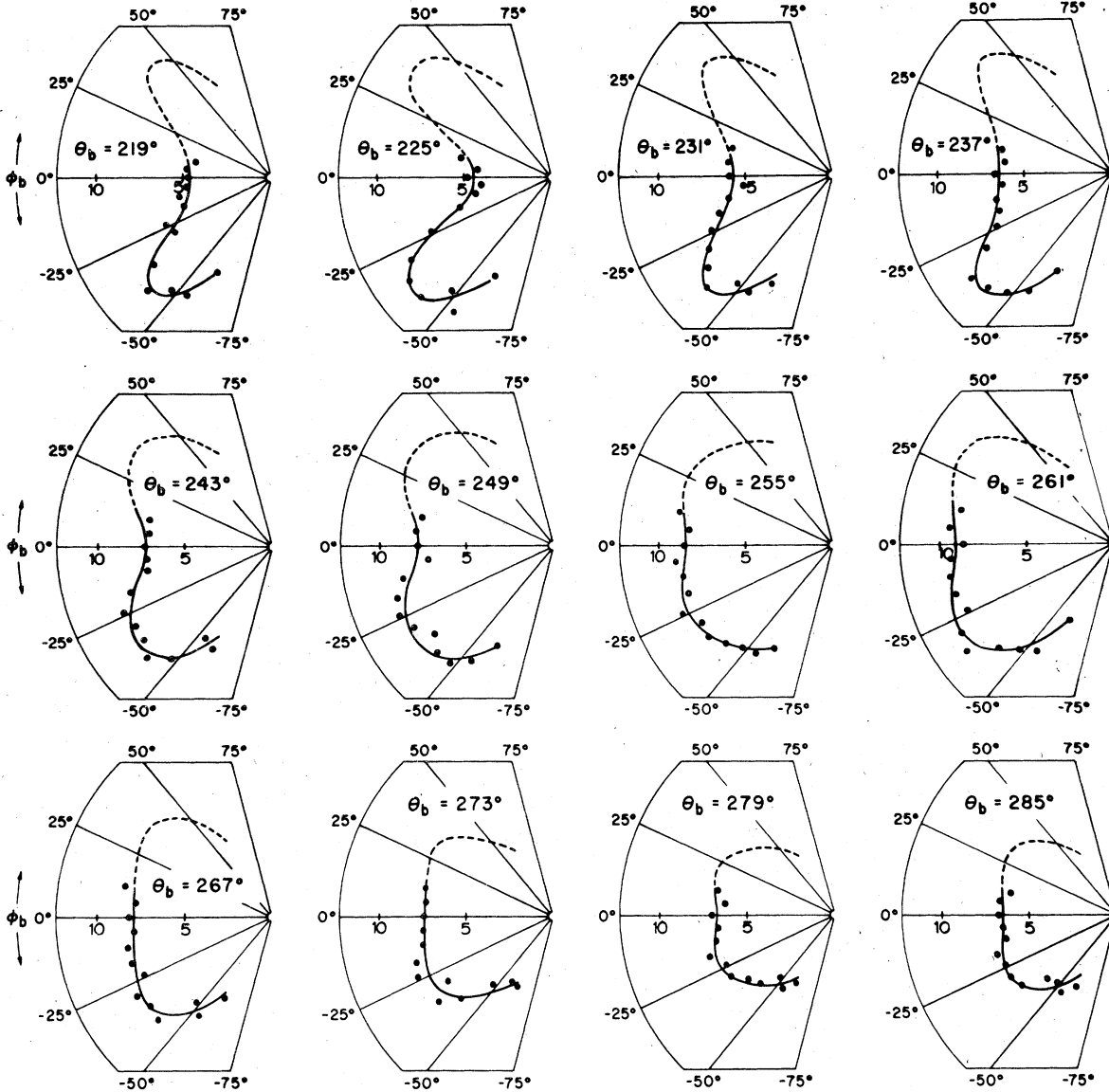


FIG. 4. Vertical scans of the backward lobe with θ_b from 219° to 285° in every 6° interval for the same case as Fig. 3. Units are the same as in Fig. 2.

set at 15° and the scattered-electron energy is fixed at 79.24 eV.

According to a simple impulse-approximation model²⁰ for certain fixed momentum transfer, \vec{K} ($=\vec{k}_0 - \vec{k}_a$), the triple-differential cross section is directly proportional to the square of the wave function in the momentum space of the ejected electron before the collision, $F(\vec{q})$,

$$\frac{d^3\sigma}{d\Omega_a d\Omega_b dE} \propto \sigma_{\text{Mott}} |F(\vec{q})|^2,$$

where σ_{Mott} is the Mott cross section and $\vec{q} = \vec{k}_0 - \vec{k}_a - \vec{k}_b$. $|F(\vec{q})|^2$ has been calculated in the Har-

tree-Fock scheme for an argon $3p$ wave function, and shown to have a maximum at $q \approx 0.65$ a.u.^{4,35} For the first set of energy variables, the minimum q , q_{min} , occurs around 0.5 a.u. Therefore from the impulse-approximation model the forward lobe of the triple-differential cross section is expected to be cylindrically symmetric about q_{min} with a minimum at the center. Ehrhardt *et al.*⁴ have already observed a minimum in the forward lobe from the in-plane measurements. For the second set of chosen energy variables, q_{min} occurs around 0.71 a.u., which means that no minimum is expected to be observed.

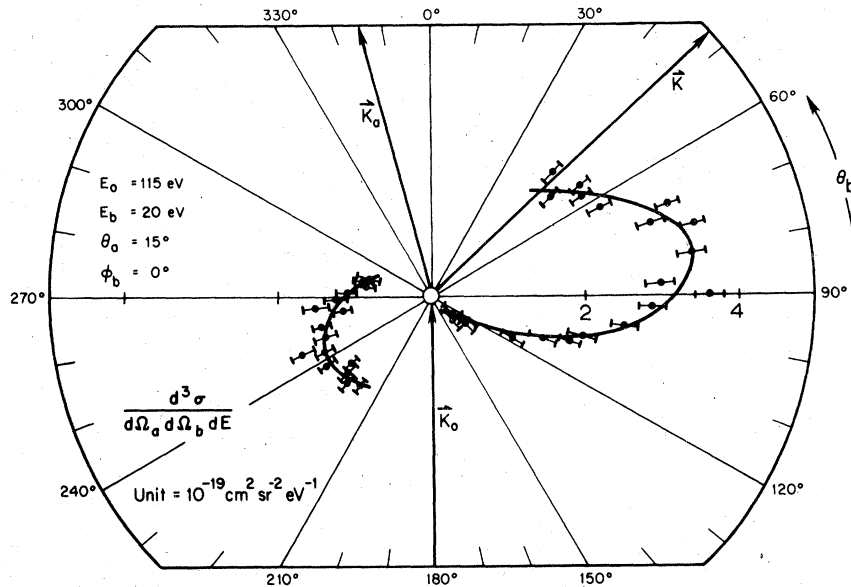


FIG. 5. In-plane measurements plotted same as Fig. 2 for the case where $E_0 = 115$ eV, $E_b = 5$ eV, and $\theta_a = 15^\circ$.

The data presented here have been put onto an absolute scale by normalizing to the absolute elastic scattering cross section of argon for scattered-electron energy of 79.24 eV and scattering angle 15° . ($\sigma_{el} = 5.08 \times 10^{-16}$ cm² sr⁻¹ is interpolated from Vuskovic and Kurepa's measurement.³⁴) The normalization procedures have already been described¹⁵; we will not repeat the description here.

The measured triple-differential cross sections as a function of the angles θ_b and ϕ_b of the ejected electron are presented in polar diagrams. Figure 2 shows the in-plane scan ($\phi_b = 0$) for the first set of data. The dots are the experimental results and the solid curve is the line fitting these data points. The error bars denote one standard deviation. Arrows \vec{k}_0 , \vec{k}_a , and \vec{K} represent the directions of incident- and scattered-electron momenta and momentum transfer, respectively. The in-plane distribution is characterized by a pronounced minimum in the forward lobe which agrees very well with the data of Ehrhardt *et al.*⁴ Furthermore, the backward peak is relatively narrower compared to the helium case where the backward peak is always found to be much broader.

In order to construct a three-dimensional picture of the triple-differential cross section, vertical scans are made; that is, θ_b is kept constant and only ϕ_b is varied in each scan. Figure 3 shows the vertical scans of the forward lobe with θ_b from 51° to 135° at 6° intervals. After averaging large amounts of data taken near the scattering plane it has been shown that the shape of the cross section is symmetric about the scattering plane. The

dotted lines are added due to this symmetry. The minimum of the forward lobe of the in-plane scan occurs at $\theta_b = 75^\circ$. From the diagram of the vertical scan at $\theta_b = 75^\circ$, the minimum is indeed a minimum in the full three-dimensional sense. The vertical scans away from the minimum show that the cross section is approximately cylindrically symmetric about the minimum.

The vertical scans of the backward lobe, from $\theta_b = 219^\circ$ to 285° at 6° intervals, are shown in Fig. 4. The backward lobe has much more structure. Simple theories such as impulse and Born approximations are apparently not adequate to explain this. The maximum of the backward lobe in the in-plane scan occurs at θ_b near 261° . From the vertical scan at $\theta_b = 261^\circ$, the maximum point in the plane in fact is a minimum point in the vertical scan. In other words it is a saddle point. It is even more surprising that there are two more lobes whose maxima point at ϕ_b near $\pm 40^\circ$. The shapes of these two lobes can be visualized by looking at the series of vertical scans from $\theta_b = 219^\circ$ through 261° . Such a structure should provide an interesting test case for any theory of ionization. As seen from Fig. 4, no simple symmetry has been found. Hence it is virtually impossible to map the whole five-dimensional space even for a limited energy range.

Results of our second set of measurements are presented in Figs. 5–7. In Fig. 5 similar to Fig. 2, the in-plane scan results are presented as a function of θ_b . The forward peak indeed does not have a minimum. The simple impulse approxima-

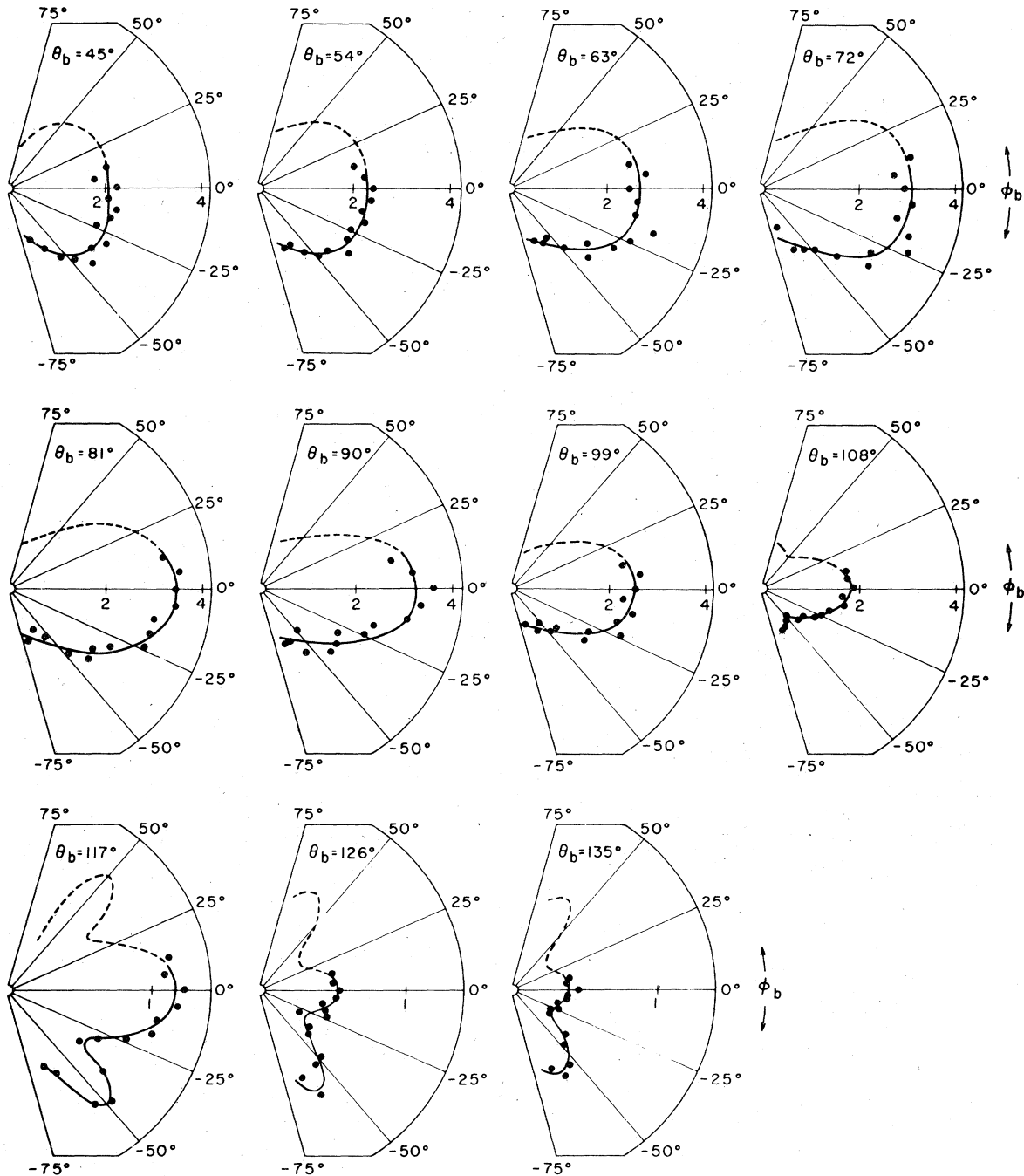


FIG. 6. Vertical scans of the forward lobe with θ_b from 45° to 135° in every 9° interval for the case where $E_b = 11$ eV, $E_a = 20$ eV, and $\theta_a = 15^\circ$. The scale has been enlarged for angular plots of vertical scans at $\theta_b = 117^\circ$, 126° , and 135° . Units are the same as in Fig. 5.

tion model gives a rather good qualitative description of the shape of the forward lobe.

The vertical scans were made for the forward and backward lobes with θ_b 9° apart. They are shown in Figs. 6 and 7, respectively. The appar-

ent maximum in the plane appears at θ_b about 81° . The vertical scan at $\theta_b = 81^\circ$ shows that it is a maximum in the three-dimensional sense. From the vertical scans away from $\theta_b = 81^\circ$, the forward lobe is obviously not cylindrically symmetric

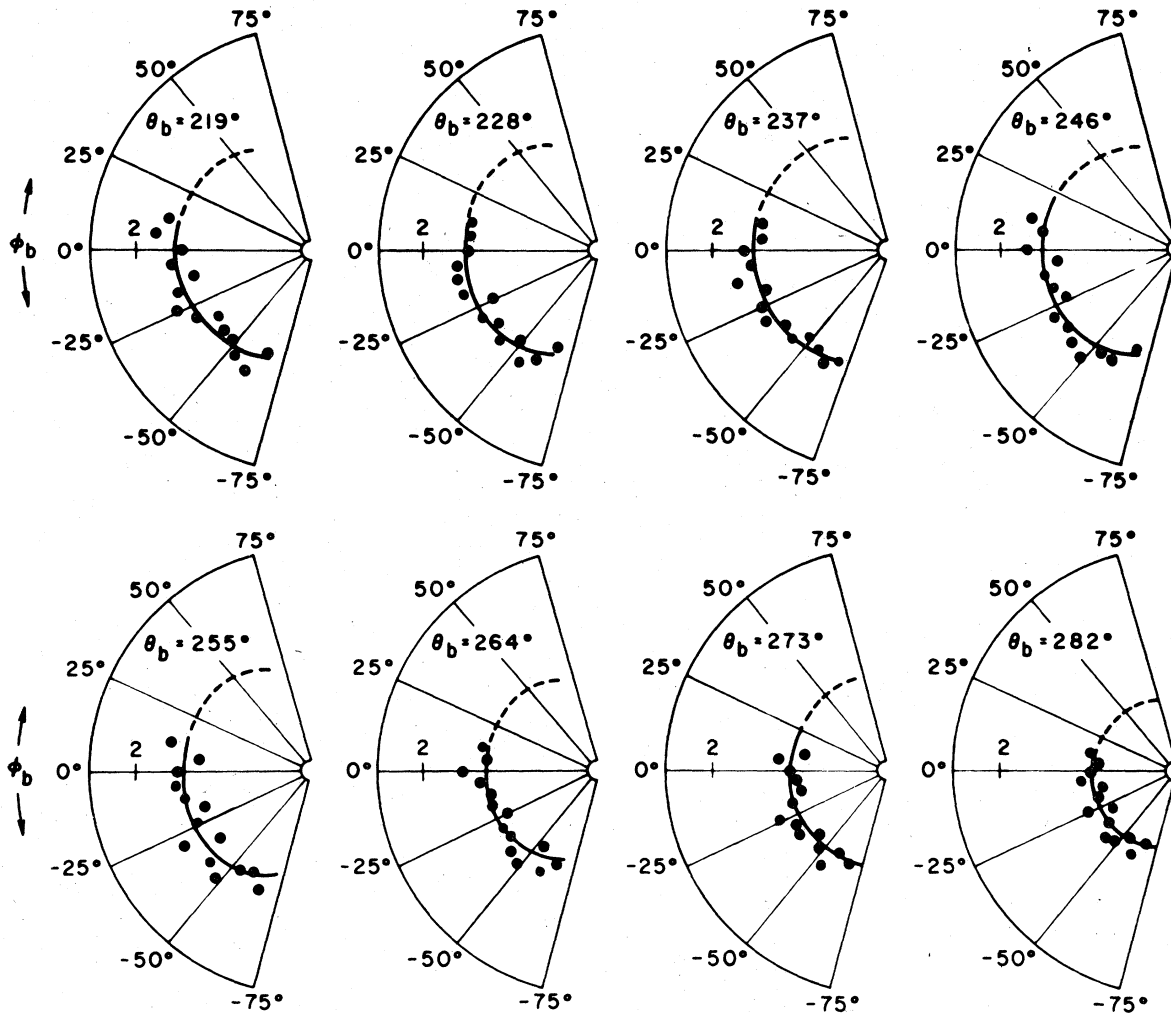


FIG. 7. Vertical scans of the backward lobe with θ_b from 219° to 282° in every 9° interval for the same case as Fig. 6. Units are the same as in Fig. 5.

about the maximum. Other structures have appeared in the vertical scans at $\theta_b = 108^\circ$ – 135° . These again cannot be explained by either the impulse-approximation model or the Born approximation. From Fig. 7, we see that the backward peak in this set of measurements is rather smooth. From all the vertical scans, the backward lobe is even closer to being spherically symmetric.

IV. CONCLUSIONS

The triple-differential cross section of the outer-shell ionization of argon has been measured for two cases. The in-plane and the out-of-plane measurements in this work will help to visualize the three-dimensional shape of the triple-differential cross section of argon. For the case where E_0

$= 100$ eV, $E_b = 5$ eV, and $\theta_a = 15^\circ$, the forward lobe of the triple-differential cross section is approximately cylindrically symmetric about an axis in the scattering plane along the direction of $\theta_b = 75^\circ$. A minimum in the three-dimensional sense has been found. The backward lobes have more structures which cannot be predicted by simple impulse approximation or Born approximation. For the case where $E_0 = 115$ eV, $E_b = 20$ eV, and $\theta_a = 15^\circ$, the results of the vertical scans show that the forward lobe is not cylindrically symmetric about any axis. More-sophisticated theory will be necessary to explain the experimental results.

ACKNOWLEDGMENTS

We would like to thank P. J. O. Teubner for his comments on the manuscript.

- *Staff member, Quantum Physics Division, National Bureau of Standards.
- ¹H. Ehrhardt, K. H. Hesselbacher, K. Jung, and K. Willmann, *Case Stud. At. Phys.* **2**, 159 (1971).
 - ²H. Ehrhardt, K. H. Hesselbacher, K. Jung, and K. Willman, *J. Phys. B* **5**, 1559 (1972).
 - ³H. Ehrhardt, K. H. Hesselbacher, K. Jung, M. Schulz, and K. Willmann, *J. Phys. B* **5**, 2107 (1972).
 - ⁴H. Ehrhardt, K. H. Hesselbacher, K. Jung, E. Schubert, and K. Willmann, *J. Phys. B* **7**, 69 (1974).
 - ⁵K. Jung, F. Schubert, D. A. L. Paul, and H. Ehrhardt, *J. Phys. B* **8**, 1330 (1975).
 - ⁶K. Jung, E. Schubert, H. Ehrhardt, and D. A. L. Paul, *J. Phys. B* **9**, 75 (1976).
 - ⁷E. Schubert, A. Schuck, K. Jung, and H. Ehrhardt, in *Tenth International Conference on the Physics of Electronic and Atomic Collisions, Abstracts of Papers*, edited by M. Barat and J. Reinhardt (Comisariat à l'Energie Atomique, Paris, 1977), p. 1066.
 - ⁸S. T. Hood, I. E. McCarthy, P. J. O. Teubner, and E. Weigold, *Phys. Rev. A* **8**, 2494 (1973).
 - ⁹S. T. Hood, I. E. McCarthy, P. J. O. Teubner, and E. Weigold, *Phys. Rev. A* **9**, 260 (1974).
 - ¹⁰E. Weigold, S. T. Hood, and I. E. McCarthy, *Phys. Rev. A* **11**, 566 (1975).
 - ¹¹A. Ugbabe, E. Weigold, and I. E. McCarthy, *Phys. Rev. A* **11**, 576 (1975).
 - ¹²E. Weigold, A. J. Dixon, I. E. McCarthy, and C. J. Noble, in Ref. 7, p. 364.
 - ¹³E. Weigold, I. Fuss, I. E. McCarthy, and C. J. Noble, in Ref. 7, p. 366.
 - ¹⁴C. E. Brion, S. T. Hood, A. Hamnett and J. Cook, in Ref. 7, p. 380.
 - ¹⁵E. C. Beaty, K. H. Hesselbacher, S. P. Hong, and J. H. Moore, *J. Phys. B* **10**, 611 (1977).
 - ¹⁶E. C. Beaty, K. H. Hesselbacher, S. P. Hong, and J. H. Moore, *Phys. Rev. A* (to be published).
 - ¹⁷E. C. Beaty, K. H. Hesselbacher, S. P. Hong, and J. H. Moore, in Ref. 7, p. 374.
 - ¹⁸R. Camilloni, A. Giardini-Guidoni, R. Tirribelli, and G. Stefani, *Phys. Rev. Lett.* **29**, 618 (1972).
 - ¹⁹M. A. Coplan, E. C. Brooks, III, and J. H. Moore, in Ref. 7, p. 378.
 - ²⁰A. E. Glassgold and G. Ialongo, *Phys. Rev.* **175**, 151 (1968).
 - ²¹L. Vriens, *Physica* **49**, 602 (1970).
 - ²²A. Giardini-Guidoni, G. Missoni, R. Camilloni, and G. Stefani, in *Electron and Photon Interactions with Atoms*, edited by H. Kleinpoppen and M. R. C. McDowell (Plenum, New York, 1976), pp. 149-160.
 - ²³A. Salin, *J. Phys. B* **6**, L 34 (1973).
 - ²⁴M. Schulz, *J. Phys. B* **6**, 2580 (1973).
 - ²⁵V. L. Jacobs, *Phys. Rev. A* **10**, 499 (1974).
 - ²⁶T. Burnett, S. P. Rountree, G. Doolen, and W. D. Robb, *Phys. Rev. A* **13**, 626 (1976).
 - ²⁷V. G. Levin, V. G. Neudatchin, A. V. Pavlitchenkov, and Yu. F. Smirnov, *J. Chem. Phys.* **63**, 1541 (1975).
 - ²⁸J. B. Furness and I. E. McCarthy, *J. Phys. B* **7**, 541 (1974).
 - ²⁹S. Geltman and M. B. Hidalgo, *J. Phys. B* **7**, 831 (1974).
 - ³⁰S. Geltman, *J. Phys. B* **7**, 1994 (1974).
 - ³¹D. H. Phillips and M. R. C. McDowell, *J. Phys. B* **6**, L165 (1973).
 - ³²K. L. Baluja and H. S. Taylor, *J. Phys. B* **9**, 829 (1976).
 - ³³D. H. Madison, R. V. Calhoun, and W. N. Shelton, *Phys. Rev. A* **16**, 552 (1977).
 - ³⁴L. Vuskovic and M. V. Kurepa, *J. Phys. B* **9**, 837 (1976).
 - ³⁵E. Clementi, *IBM J. Res. Dev.* **9**, Table 30-01, 31-01 (1965).